

On the transition to self-gravity in low mass AGN and YSO accretion discs

Jean-Marc Huré^{1,2}

¹DAEC et UMR 8631 du CNRS, Observatoire de Paris-Meudon, Place Jules Janssen, 92195 Meudon Cedex, France

²Université Paris 7 (Denis Diderot), 2 Place Jussieu, 75251 Paris Cedex 05, France

Received 31 March 2000 / accepted 11 April 2000

Abstract. The equations governing the vertical structure of a stationary keplerian accretion disc supporting an Eddington atmosphere are presented. The model is based on the α -prescription for turbulent viscosity (two versions are tested), includes the disc vertical self-gravity, convective transport and turbulent pressure. We use an accurate equation of state and wide opacity grids which combine the Rosseland and Planck absorption means through a depth-dependent weighting function. The numerical method is based on single side shooting and incorporates algorithms designed for stiff initial value problems. A few properties of the model are discussed for a circumstellar disc around a sun-like star and a disc feeding a $10^8 M_{\odot}$ central black hole. Various accretion rates and α -parameter values are considered.

We show the strong sensitivity of the disc structure to the viscous energy deposition towards the vertical axis, specially when entering inside the self-gravitating part of the disc. The local version of the α -prescription leads to a "singular" behavior which is also predicted by the vertically averaged model: there is an extremely violent density and surface density runaway, a rapid disc collapse and a temperature plateau. With respect, a much softer transition is observed with the " $\alpha\mathcal{P}$ -formalism". Turbulent pressure is important only for $\alpha \gtrsim 0.1$. It lowers vertical density gradients, significantly thickens the disc (increases its flaring), tends to wash out density inversions occurring in the upper layers and pushes the self-gravitating region to slightly larger radii. Curves localizing the inner edge of the self-gravitating disc as functions of the viscosity parameter and accretion rate are given. The lower α , the closer to the center the self-gravitating regime, and the sensitivity to the accretion rate is generally weak, except for $\alpha \gtrsim 0.1$.

This study suggests that models aiming to describe T-Tauri discs beyond about a few to a few tens astronomical units (depending on the viscosity parameter) from the central protostar using the α -theory should consider vertical self-gravity, but additional heating mechanisms are necessary to account for large discs. The Primitive Solar Nebula was probably a bit (if not strongly) self-gravitating

at the actual orbit of giant planets. In agreement with vertically averaged computations, α -discs hosted by active galaxies are self-gravitating beyond about a thousand Schwarzschild radii. The inferred surface density remains too high to lower the accretion time scale as requested to fuel steadily active nuclei for a few hundred millions years. More efficient mechanisms driving accretion are required.

Key words: Accretion, accretion disks – Equation of state – Solar system: formation – Galaxies: active – Galaxies: nuclei

1. Introduction

Viscous discs can acquire large dimensions under the effect of angular momentum redistribution. This is corroborated by the observation of Young Stellar Objects (YSO) which reveals the emission of wide gaseous discs with an outer radius reaching 100 – 1000 AU (Beckwith et al., 1990; Pudritz et al., 1996; Duvert et al., 1998; Guilloteau & Dutrey, 1998; Shepherd & Kurtz, 1999). Also, discs hosted by Active Galactic Nuclei (AGN), although yet unresolved—except in the active galaxy NGC4258 (Herrnstein et al., 1999)—could probably be of much larger size. The existence of strong similarities between YSOs and AGNs, like jets and outflows (Falcke, 1998; Frank, 1998), some excesses in the spectral energy distribution at infrared wavelengths (Adams & Shu, 1986; Zdziarski, 1986; Bertout, 1989; Sanders et al., 1989; Voit 1991; Kenyon, Yi & Hartmann, 1996), a surrounding (dusty) torus (Güsten, Chini & Neckel, 1984; Thé & Molster, 1994; Drinkwater, Combes & Wiklind, 1996; Sandqvist, 1999) indicates that the same physical mechanisms should take place in discs, despite the difference in the central mass scale. This constitutes an interesting challenge for the disc theory, especially to understand the transport of angular momentum.

Many models are based on the α -theory of thin discs (Shakura & Sunyaev, 1973; Pringle, 1981) and assume a vertically averaged structure (e.g., Collin & Dumont 1990; Ruden & Pollack, 1991; Cannizzo & Reiff, 1992; Huré et al. 1994a; Artemova et al. 1996; Burderi, King

& Szuszkiewicz, 1998; Drouart et al. 1999; Aikawa et al., 1999). A physically more satisfactory approach is the investigation of the vertical structure in detail, as done for stars. Such a problem has been discussed by several groups already, in different contexts, with various goals and degrees of sophistication: at the scale of AGNs (Cannizzo, 1992; Wehrse, Störzer & Shaviv, 1993; Dörrer et al., 1996; Siemiginowska, Czerny & Kostyunin, 1996; Hubeny & Hubeny, 1998 and references therein; Sincell & Krolik, 1997; Różańska et al., 1999), in Cataclysmic Variables (CVs) (Smak, 1984; Mineshige & Osaki, 1983; Meyer & Meyer-Hofmeister, 1982; Pojmański, 1986; see Cannizzo, 1993 for a review; Milsom, Chen & Taam, 1994; Dubus et al., 1999) and in YSOs (Malbet & Bertout, 1991; Bell et al., 1997; D’Alessio et al., 1998) including the Primitive Solar Nebula (PSN) (Lin & Papaloizou, 1980; Papaloizou & Terquem, 1999). Basic considerations show that the outermost regions of (low mass) discs are expected to be regulated by self-gravity (Goldreich & Lynden-Bell, 1965; Shlosman & Begelman, 1987). This may be the case of AGN and YSO discs. A few constraints on the disc thickness, mass and rotation motion at large radii are set by observations (Guilloteau & Dutrey, 1998; Mundy, Looney & Welch, 2000; Herrnstein et al., 1999). So, it appears essential to construct models for as accurate and realistic as possible, despite the lack of knowledge regarding turbulent viscosity which causes accretion. To our knowledge, no self-consistent 2D-model accounting for vertical self-gravity in the outermost parts of discs has been published yet. This is the aim of this paper. The present model includes simultaneously vertical convection, self-gravitation, turbulent pressure, and realistic equation of state (EOS) and opacities. Of particular interest here is the transition from the “classical” disc to the self-gravitating disc which is predicted to be as close as a few $10^3 - 10^4 R_*$ (R_* is the radius of the central object) by vertically averaged models (Ruden & Pollack, 1991; D’Alessio, Calvet & Hartmann, 1997; Huré, 1998). The hypothesis of the model and relevant equations are developed in Sect. 2. Two versions of the α -prescription are tested. The ingredients (EOS and opacities) as well as the numerical method are presented in Sect. 3. We discuss in Sect. 4 a few properties of the model, namely the effect of turbulent pressure and depth dependent viscosity, and the position of the inner edge of the self-gravitating disc, for prototypal circumstellar and AGN discs, for various accretion rates. An Appendix contains a note concerning the treatment of convection and a high precision formula fitting the EOS.

2. Model for the vertical structure: hypothesis and relevant equations

2.1. General considerations. Accounting for self-gravity

A distinctive feature of steady state keplerian accretion discs is the absence of coupling between the vertical structure and the radial structure (e.g. Frank, King & Raine,

1992). This attractive property is undoubtedly an oversimplification and probably does not match reality. However, it is particularly advantageous from a modeling point of view because any annulus can be treated individually, whatever the state of neighbors, unlike in thick discs where pressure gradients and energy transport in the radial direction gain in importance with respect to their vertical counterparts (Maraschi, Reina & Treves, 1976; Abramowicz, Calvani & Nobili, 1980; Abramowicz et al., 1988; Narayan, Madevan & Quataert, 1998). Note that the keplerian assumption which fixes the rotation law to the value

$$\Omega = \sqrt{\frac{GM}{R^3}} \quad (1)$$

where M is the central mass and R the polar radius, requires that the gas remains confined at altitudes z such as $z^2 \ll R^2$, and small radial pressure gradients too.

Self-gravity may influence and even dominate the equilibrium structure and dynamical evolution of almost any kind of disc, not only in massive or thick discs or tori where effects are global (Bodo & Curir, 1992; Hashimoto, Eriguchi, Müller, 1995; Boss, 1996; Laughlin & Różyczka, 1996; Masuda, Nishida & Eriguchi, 1998), but also in low mass keplerian discs (Paczyński, 1978; Shlosman & Begelman, 1987) as soon as the mass density of the accreted gas exceeds $\sim \Omega^2/4\pi G$ locally, Ω being the rotation frequency. In that latter case which is of interest here, self-gravity increases vertical pressure gradients and gathers matter closer to the midplane (Sakimoto & Coroniti, 1981; Shore & White, 1982; Cannizzo & Reiff, 1992; Huré et al., 1994; Huré, 1998). So, only the outermost regions of keplerian discs where Ω reaches low values can be affected by vertical self-gravity, except in very special situations (e.g. Sincell & Krolik, 1997).

Accounting correctly for the disc gravity requires the resolution of the Poisson equation (Hunter, 1963; Störzer, 1993; Bertin & Lodato, 1999)

$$\Delta\Phi^{\text{disc}}(R, z) = -4\pi G\rho(R, z) \quad (2)$$

where ρ is the gas mass density and Φ^{disc} is the gravitational potential due to the bare disc (the ϕ -invariance is assumed). This is a very difficult task, in particular because the disc surface has a non trivial form which is not known a priori and the deviation from sphericity is extreme. As Eq.(2) connects all annuli together, the method of “independent rings” no longer applies, unless an iterative scheme in which the potential would be step by step improved from the actual density field until convergence (Stahler, 1983). There is however no guarantee that such a scheme effectively converge and the computational time might be prohibitive (Eriguchi & Müller, 1991). Here, we follow another, more simple approach: we adopt the infinite and R -homogeneous slab approximation (Paczyński, 1978; Sakimoto & Coroniti, 1981; Shore & White, 1982;

Cannizzo & Reiff, 1992; Liu, Xie & Ji, 1994; Huré, 1998) which yields the gravity due to the disc

$$g_z^{\text{disc}}(R, z) = \frac{\partial \Phi^{\text{disc}}}{\partial z} \approx -4\pi G \Sigma(R, z), \quad (3)$$

where the surface density Σ is defined by

$$\Sigma(R, z) = \int_0^z \rho(R, z') dz', \quad (4)$$

but other assumptions are possible (Mineshige & Umemura, 1997). This enables again to investigate the disc structure annulus by annulus, but introduces a bias: it tends to overestimate (underestimate) self-gravity in regions of high (respectively low) densities. We expect that the present approximation gives acceptable results, at least in regions where the surface density radial gradients remain low with respect to density. Anyway, the error made with respect to a self-consistent model is not known and would be interesting to estimate.

2.2. The equations for the disc interior

When the upward transport of heat is treated in the diffusion approximation, the vertical structure of a keplerian disc, possibly irradiated, can be determined from the resolution of a system of four first order coupled ordinary differential equations (ODEs) in between the midplane and the top of the disc (Pojmański, 1986; Tuchman, Mineshige & Wheeler, 1990; Cannizzo, 1992; Meyer & Meyer-Hofmeister, 1982; Milsom, Chen & Taam, 1994; Dubus et al., 1999). The complexity of the problem rises when a multi-frequency radiative transfer is performed, as required to compare theoretical spectra with observations and make key predictions (Ross, Fabian & Mineshige, 1992; Wehrse, Störzer & Shaviv, 1993; Dörrer et al., 1996; Sincell & Krolik, 1997; D’Alessio et al. 1998; El-Khoury & Wickramasinghe, 1998; Hubeny & Hubeny, 1998; De Kool & Wickramasinghe, 1999). The four equations specify respectively (Frank, King & Raine, 1992):

- the pressure gradient $\nabla_z P$ which describes the hydrostatic equilibrium of each fictitious slab

$$\frac{1}{\rho} \frac{dP}{dz} = -\Omega^2 z - 4\pi G \Sigma \equiv g_z, \quad (5)$$

- the heat flux gradient $\nabla_z F$ due to viscous heating

$$\frac{dF}{dz} = \frac{9}{4} \rho \nu \Omega^2, \quad (6)$$

where ν is the z -dependent viscosity law (see Sect. 2.4),

- the temperature gradient $\nabla_z T$ which is determined by the heat net flux transported upwards through radiation and convection

$$\frac{dT}{dz} = -T \frac{\nabla}{\lambda_p}, \quad (7)$$

where $\lambda_p \equiv -\frac{dz}{d \ln P}$ is the pressure height scale and $\nabla \equiv \frac{d \ln T}{d \ln P}$ is the actual gradient (see the Appendix, Sect. A),

- the surface density gradient $\nabla_z \Sigma$

$$\frac{d\Sigma}{dz} = \rho \quad (8)$$

Note that this last equation is not relevant when self-gravity is left apart (the total surface density of the disc + atmospheres $\Sigma_t = 2 \times \Sigma(R, \infty)$ can be easily computed a posteriori from Eq.(4), once the mass density distribution is known). The above ODEs must be supplemented by a closure relation, an equation of state. For a mixture of radiation and perfect gas undergoing atomic ionization and molecular dissociation at LTE, the total pressure is linked to the density and temperature of matter by

$$P = \frac{\rho k T}{\mu m_H} + \frac{4 \sigma}{3 c} T^4 \quad (9)$$

where μm_H is the mean mass per particle which depends on the density and temperature (see Sect. 3.1 and the Appendix, Sect. B). The above expression for radiation pressure is compatible with an optically thick disc only.

2.3. Accounting for turbulent pressure in the framework of the α -prescription

Turbulence is the main mechanism driving accretion in discs. It is an extra source of pressure. According to the standard theory of α -discs (Shakura & Sunyaev, 1973; Pringle, 1981), the typical velocity of turbulent eddies can be taken as $\sim \sqrt{\alpha} c_s$ if one assumes the equipartition between length and velocity turbulent scales (c_s is the adiabatic sound speed). So, the turbulent pressure is

$$p_t = \alpha \Gamma_1 P \quad (10)$$

where $\Gamma_1 = \left(\frac{d \ln P}{d \ln \rho}\right)_{\text{ad}}$ is the first adiabatic exponent in the total (gas plus radiation) pressure. The effect of turbulent pressure on the hydrostatic equilibrium is therefore expected if α is not too small, as simulations shall confirm. If we include p_t into Eq.(5) and rewrite it in terms of a density gradient equation, we find

$$\frac{d\rho}{dz} = -\frac{\rho^2}{P} (\Omega^2 z + 4\pi G \Sigma) \frac{1 - \chi_T \nabla}{\chi_\rho (1 + \alpha \Gamma_1)} \quad (11)$$

where χ_T and χ_ρ are respectively the temperature and density exponents of the total pressure, and we have assumed $\nabla_z \Gamma_1 = 0$ (this is justified since $0.9 \lesssim \Gamma_1 \lesssim 1.7$, see for instance the Appendix, Fig.(A.1)). This expression clearly shows the existence of a density inversion (that is, a zone where $\nabla_z \rho > 0$) each time the actual gradient satisfies $\chi_T \nabla > 1$ (Różańska et al., 1999). Such an inversion is likely to occur in radiative pressure dominated layers where χ_T is the largest or/and in convectively unstable zones where ∇ may be large. Note that the inversion

still remains if turbulent pressure plays a role, but with a weaker amplitude.

It is likely that turbulent pressure plays a role, not only on the hydrostatic equilibrium as considered here, but also on advection of matter and energy both radially and vertically. We ignore these effects.

2.4. On depth-dependent viscosity laws

In vertically averaged disc models, the anomalous viscosity takes locally a mean value defined from midplane quantities, namely $\nu \equiv \nu^{\text{midplane}} (= \alpha c_s^2(0)/\Omega)$. Here, we need to specify how ν varies with the altitude. This point is critical since our knowledge of turbulent viscosity remains extremely limited, if not null. There are however two standard ways to do this within the framework of the α -prescription. The most common one is to assume that the shear stress is proportional to some pressure (the so-called " $\alpha\mathcal{P}$ -formalism"; e.g. Cannizzo, 1992). It leads to a viscosity law

$$\nu_1 = \frac{2\alpha\mathcal{P}}{3\Omega\rho} \equiv \nu_1(R, z) \quad (12)$$

where \mathcal{P} can be either gas pressure, or total pressure or some combination of the two (Siemiginowska, Czerny & Kostyunin, 1996; Artemova et al., 1996; Hameury et al., 1998; Papaloizou & Terquem, 1999), with different consequences on the disc stability (Camenzind, Demole & Straumann 1986; Clarke, 1988). The other way uses the local version of the α -prescription (Meyer & Meyer-Hofmeister, 1982)

$$\nu_2 = \alpha c_s \bar{\lambda}_p \equiv \nu_2(R, z) \quad (13)$$

where $\bar{\lambda}_p$ is the reduced pressure height scale (see the Appendix, Sect. A). Whatever the expression the authors adopt, the α -parameter is most often assigned to a fixed value in a disc. However, theoretical arguments, numerical simulations as well as observational constraints indicate that α should vary, not only with the radius (Shakura & Sunyaev, 1973; Cannizzo, 1993; Lasota & Hameury, 1998), but also with the altitude via the temperature or density, or other quantities (Brandenburg, 1998). Strictly speaking, the need for strong variations of the α -parameter means the failure of the α -viscosity model.

Since ν_1 and ν_2 are formally different, even with the same α -parameter, they lead to different vertical structures and consequently to different discs, as we shall see below. Besides, the correspondence between the two laws (a multiplying factor $\frac{3}{2}\Omega\lambda_p\Gamma_1/c_s$ from ν_1 to ν_2 , if $\mathcal{P} \equiv P$) is much more subtle than shifting α : in general, $\Omega\lambda_p \neq c_s$ at any altitude (this is specially true at the equatorial plane where $\lambda_p \rightarrow \infty$; see Sect. 4.3). The volumic energy production associated to ν_2 is

$$\frac{dF}{dz} = \frac{9}{4}\Omega^2\lambda_p\alpha\sqrt{\Gamma_1 P\rho}, \quad (14)$$

Note that both Eqs.(12) and (13) satisfy $\frac{d\nu}{dz} < 0$ above the equatorial plane, meaning that the gas is accreted much faster at the equatorial plane than at the top of the disc. So, these laws implicitly suggest the existence a plan parallel shear which might be able to trigger turbulence and to expand turbulent eddies in the radial direction.

There are still no physical arguments to decide if ν_2 is better than ν_1 . That is why we use both expressions in the following (in particular, for ν_1 we take $\mathcal{P} \equiv P$). In fact, a wide class of functions $\nu(R, z)$ should be considered and their effects compared. It is possible that turbulent viscosity shows a weaker dependence with z than considered so far and even does not depend on the altitude at all. This is precisely the case with the β -viscosity prescription which is suggested by laboratory experiments (Pringle & Rees, 1972; Lynden-Bell & Pringle, 1974; Richard & Zahn, 1999; Duschl, Biermann & Strittmatter, 2000; Huré, Richard & Zahn, 2000).

2.5. Equations for the Eddington atmosphere

In the Eddington approximation, the structure of the atmosphere is governed by three (only two in the absence of self-gravity) first orders ODEs. Two of these (namely Eqs.(5) and (8)) are basically the same as for the disc interior, and the third one controls the optical depth τ in the atmosphere

$$\frac{d\tau}{dz} = -\kappa\rho \quad (15)$$

where κ is a grey absorption coefficient. In order to prevent any temperature runaway which would lead to the formation of a hot corona (Shaviv & Wehrse, 1991; Różańska et al., 1999), we assume that there is no viscous energy generation in this layer and no active turbulence. It means that the atmosphere is not accreted. We are aware that the validity of all these approximations, including the Eddington approximation, is easily open to criticism. The temperature within the atmosphere follows the law (Michalás, 1978)

$$T^4 = \frac{3}{4}T_{\text{eff}}^4 \left(\tau + \frac{2}{3} \right) \quad (16)$$

where $\tau \leq \frac{2}{3}$ and T_{eff} is the effective temperature which is fixed by the outgoing flux due to internal and external heating sources, at the photosphere's base. Actually, the global effect of the disc irradiation can be taken into account at this level by a suitable definition of T_{eff} (Kenyon & Hartmann, 1987; Hubeny, 1990; Robinson, Marsh & Smak, 1993; Dubus et al., 1999). We see from Eqs.(5), (15) and (16) that the density gradient is

$$\frac{d\rho}{dz} = -\frac{\rho^2}{\chi_\rho P} (\Omega^2 z + 4\pi G\Sigma) + \frac{\chi_T \kappa \rho}{4\chi_\rho (\tau + \frac{2}{3})} \quad (17)$$

and may also become positive. As suggested above, we do not take into account turbulent pressure in this layer. This

induces a discontinuity in the density (or gas pressure) gradient at the altitude where the disc and its atmosphere join together, but not in the density itself.

2.6. Boundary conditions and matching conditions at the disc/atmosphere interface

There are two problems to solve simultaneously: the structure of the disc interior from Eqs.(6)(7)(8) and (11) and the structure of its atmosphere from Eqs.(8)(15) and (17). These differential equations are subject to Dirichlet boundary conditions. At the midplane, the symmetry imposes $\Sigma = 0$ and $F = 0$ like for a star. At the top atmosphere located at $z = H$ (to be determined), conditions are $P = P_{\text{amb}}$ the ambient pressure (which may include the pressure due to external illumination), $\tau = 0$ and $\Sigma = \frac{1}{2}\Sigma_{\text{t}}$, half the total surface density of the disc and atmosphere. Some authors specify the density (for instance $\rho \rightarrow 0$) instead of the pressure at the boundary (e.g. Pojmański, 1986; Dörrer et al. 1993; El-Khoury & Wickramasinghe, 1999). We choose a value typical of the interstellar medium, namely $P_{\text{amb}}/k = 10^5 \text{ K.cm}^{-3}$ (Duley & Williams, 1988), significantly smaller than in D'alessio et al. (1998). At the base of the atmosphere located at $z = h$ (to be determined too), the matching conditions are $\tau = \frac{2}{3}$ and $F = \sigma T_{\text{eff}}^4$ (see Sect. 4.1).

It is worthy of note that boundary conditions at the disc surface have a very weak effect on midplane quantities as long as the disc is optically thick and has a large surface density, locally. Such an insensitivity is well known in stellar structure computations (Kippenhahn & Weigert, 1990). Let us quote also that, contrary to a general belief, models that do not consider the atmosphere and use $P = -\frac{2}{3}\frac{g_z}{\kappa}$ as a boundary condition at $z = h$ always violate the Eddington approximation since this relation does not guarantee that the atmosphere has the right optical thickness (i.e. $\frac{2}{3}$). Further, the approximation

$$\int_{P(\infty)}^{P(h)} \frac{\kappa}{g_z} dP \approx \left(\frac{\kappa}{g_z} P \right)_{z=h} \quad (18)$$

becomes bad in regions where the surface density of the atmosphere is comparable to that of the disc, when the mean absorption within the atmosphere is low, or when the disc is not optically very thick. For these reasons, we sustain the idea that the use of the Eddington approximation has sense only if the structure of the atmosphere is computed together with that of the disc interior.

3. Ingredients and computational method

3.1. Equation of state and opacities for a cosmic gas

The physical problem depends on a certain amount of thermodynamical and radiative data. For the present application, the gas has cosmic abundances and is subject

to atomic ionizations and molecular dissociations. Local Thermodynamic Equilibrium (LTE) is assumed (Huré et al., 1994b). The mean mass per particle μm_{H} , coefficients χ_T and χ_ρ , adiabatic gradient ∇_{ad} , heat capacity c_p (needed to treat convective transport) and adiabatic exponent Γ_1 have been computed accurately from chemical abundances at thermal equilibrium (Huré, 1998). Grids of data with ρ and T as the inputs have been generated. Interpolations between mesh points are performed with bicubic splines. We have computed a high precision analytical expression fitting μ (and subsequently coefficients χ_T and χ_ρ) as functions of the temperature and density with an accuracy less than 4% relative to raw data in the case of a zero metallicity gas (see the Appendix, Sect. B1). This fit can be used for a cosmic gas as well without producing important errors (since metals in a cosmic mix have very low abundances relative to hydrogen, with almost no influence on the EOS and related quantities).

Opacity is probably the most important ingredient of the model and the choice for the grey absorption coefficient κ is critical, specially near the surface (Mihalas, 1978). Here, we take (Hameury et al., 1998)

$$\kappa = \theta \kappa_{\text{R}} + (1 - \theta) \kappa_{\text{P}} \quad (19)$$

where κ_{R} and κ_{P} are the Rosseland and Planck means respectively, and θ is a function which varies continuously from 0 to 1 as the optical depth increases from 0 to infinity. A suitable choice is

$$\theta_m(\tau) = \frac{1}{1 + \tau^m} \quad (20)$$

where the index m sets the stiffness of the transition from κ_{P} to κ_{R} ($m = 1$ is taken in the following applications). The θ -function is arbitrary and should strongly influence physical quantities at the disc surface. Also, we are aware that the best grey coefficient is probably neither given by κ_{R} , nor by κ_{P} , nor by Eq.(19). A flux weighted opacity mean could be better (Mihalas, 1978; Hubeny, 1990).

Tables of Rosseland and Planck means have been taken from various sources (Pollack et al., 1994; Huré et al., 1994b; Alexander & Ferguson, 1994; Henning & Stognienko, 1996; Seaton et al., 1994). But Planck absorption means published by the Opacity Project (OP) (Seaton et al., 1996) have not been selected due to apparently large errors of unknown origin (Alexander, 1998; Zeippen, 1999). Two grids of data have been generated after passing through filters (mainly running averages) to smooth out discontinuities. Finally, opacity grids cover the temperature range $10 - 10^8 \text{ K}$ and extend from extremely high to extremely low densities where the ideal gas and LTE assumptions are expected to fail. An example of Rosseland and Planck means versus the temperature is displayed in Fig.(1). As done for the equation of state and related quantities, opacity values between mesh points are interpolated using bicubic splines. Working with analytical opacities may present some advantages (Burgers & Lamers, 1989;

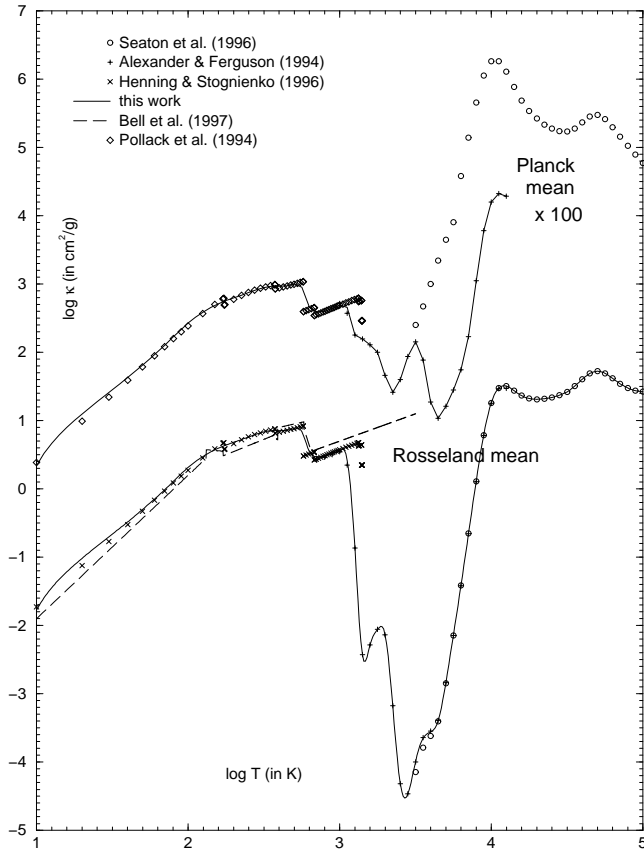


Fig. 1. Rosseland and Planck absorption coefficients versus the temperature from various sources for hydrogen and metal mass fractions $X = 0.70$ and $Z = 0.02$ respectively and $\rho = 10^{-15} \times T^3 \text{ g.cm}^{-3}$ (i.e. $\log R = -3$ in the OP format; see Seaton et al., 1994). Planck means have been shifted upwards for clarity.

Collin & Dumont, 1990; Bell & Lin, 1994), but they can also produce numerical instabilities in the integration of the disc structure equations since they mostly consist in continuous but non derivable piecewise functions.

3.2. Computational method

The altitude of the top atmosphere being not known a priori, many numerical methods for solving Two Boundary Value Problems (TBVPs) are almost unusable in the actual situation. It is however possible to apply variable changes, namely $\nabla_z \rightarrow \nabla_\tau$ in the atmosphere and $\nabla_z \rightarrow \nabla_F$ in the disc interior (Cannizzo & Cameron, 1988) in order to recover a common TBVP with fixed boundaries (e.g. $\frac{F}{\sigma T_{\text{eff}}^4} \in [0, 1]$), but this drastically increases vertical gradients near the surface and make the problem more unstable from a numerical point of view. Some groups work with relaxation algorithms (Cannizzo, 1992; Milsom, Chen & Taam, 1994; D'alessio et al., 1998; Hameury et al., 1998) which require (good) vertical profiles as starting guesses and are known to be rapidly converging methods. How-

ever, zones with steep gradients generally need a local mesh refinement. Other authors prefer straight integrators and algorithms based on shooting methods (Lin & Papaloizou, 1980; Meyer & Meyer-Hofmeister, 1982; Mineshige & Osaki, 1983; Smak, 1984; Mineshige, Tuchman & Wheeler, 1990; Róžańska et al., 1998; Papaloizou & Terquem, 1999) typical of Initial Values Problems (IVPs), with only a few quantities to guess but with possible troubles regarding the precision.

In the present case, we have written a Fortran code named **VS³KAD** which performs the integration of the disc and atmosphere equations using single side shooting and numerical routines specially designed for stiff IVPs. Integration steps are variable, internally to the routines and the accuracy can be as small as the machine precision. In its present version, the code works with the following variables: $\ln T$, $\ln \rho$, $\frac{F}{\sigma T_{\text{eff}}^4}$, $\frac{2\Sigma}{\Sigma_t}$ and τ , but more clever choices are possible, specially to reduce artificially the stiffness of the equations. We have noticed that the computational time is considerably smaller than with Runge-Kutta algorithms, even with a variable step. Like in many stiff problems, the numerical integration may turn out to be non conservative: integrating from the top atmosphere down to the midplane can give a solution which, in the surface neighborhood, can be very different than that obtained when integrating in the opposite direction (Mineshige, Tuchman & Wheeler, 1990; Press et al., 1992; De Kool & Wickramasinghe, 1999). This has been observed in the present case. It reminds the influence of both boundary conditions and underlying methodology. The best stability and reliability of the results are obtained by starting from the boundary layer where almost all the stiffness of the problem is concentrated.

In practical, given a central mass M , accretion rate \dot{M} , α -parameter, radius R and total energy deposition σT_{eff}^4 at the bottom atmosphere (see Sect. 4.1), the computation starts at an arbitrary altitude $z = H^{(0)}$ (the top atmosphere) where the surface density $\Sigma^{(0)}(H^{(0)})$ is guessed. The integration then proceeds downwards. Once the bottom atmosphere is reached, at an altitude $z = h^{(0)}$, the equations for the disc interior are integrated down to the midplane where the net flux and surface density generally differ from zero. By successive iterations on $H^{(i)}$ and $\Sigma(H^{(i)})$ —performed with a Newton-Raphson method—, quantities $F^{(i)}(0)$ and $\Sigma^{(i)}(0)$ can be driven to very small values. The problem has converged after n iterations, when simultaneously $F^{(n)}(0) \approx 0$ and $\Sigma^{(n)}(0) \approx 0$ with the requested precisions

$$-\epsilon_-^F \leq \frac{F^{(n)}(0)}{\sigma T_{\text{eff}}^4} \leq \epsilon_+^F, \quad (21)$$

$$-\epsilon_-^\Sigma \leq \frac{2\Sigma^{(n)}(0)}{\Sigma_t} \leq \epsilon_+^\Sigma \quad (22)$$

and

$$-\epsilon_-^H \leq 1 - \frac{H^{(n)}}{H^{(n-1)}} \leq \epsilon_+^H, \quad (23)$$

where ϵ_+^F , ϵ_+^H , ϵ_+^Σ , ϵ_-^Σ , ϵ_-^H and ϵ_+^H are very small, positive values. Since our treatment of self-gravity is very approximate, it is legitimate to allow a much lower (but sufficient) precision on the surface density (this accelerates convergence and lowers the computational time). On average, it takes a few milliseconds CPU on a single user personal computer and $n \lesssim 25$ with $\epsilon_0^F = \epsilon_0^H = (\epsilon_0^\Sigma)^2 = 10^{-10}$ where $\epsilon_0^F = \text{Sup}(\epsilon_-^F, \epsilon_+^F)$, $\epsilon_0^\Sigma = \text{Sup}(\epsilon_-^\Sigma, \epsilon_+^\Sigma)$ and $\epsilon_0^H = \text{Sup}(\epsilon_-^H, \epsilon_+^H)$. This precision is sufficient in most cases. When self-gravity is neglected, Eq.(8) becomes obsolete. The iteration is on the flux only and the code then runs much faster (by a factor ~ 5), with $n \lesssim 6$.

The code has been tested and compared in many situations (e.g. without self-gravity, without turbulent pressure, with and without external irradiation) with reference models (Różańska, 1998; Hameury et al., 1998) and appears to behave very well¹. It automatically scales to the central mass, and is able to model any kind of disc: AGN discs, CV discs, YSO discs and sub-nebulae as well. A simulation of D/H enrichments in the PSN with this code is currently under way (Hersant, Gautier, Huré, 2000).

4. A few applications of the model

4.1. The hypothesis of a non irradiated disc

Vertically averaged disc models show that the non self-gravitating and gas pressure dominated parts of α -discs have an aspect ratio $\frac{h}{R} \sim 0.001 - 0.1$, depending on the central mass and accretion rate mainly. There is a slight flaring (i.e. $\frac{d \ln h}{d \ln R} \gtrsim 1$) which eventually may vanish in the outermost regions (e.g. Ruden & Pollack, 1991; Bell et al., 1997). The existence of a flaring inner disc is supported by observations: the spectrum of T-Tauri stars and AGN contains a prominent infrared component which is currently interpreted as light re-processing in the superficial layers of the disc (Adams & Shu, 1986; Voit, 1991; Chiang & Goldreich, 1997). It is possible that self-irradiation also plays a role (Fukue, 1992). For circumstellar discs, the flaring angle of bare α -disc is too low to enhance the infrared spectral component to the observed level (Kenyon & Hartmann, 1987). And the heating by the central star should not produce a significant increase of the flaring (e.g. D'alessio et al., 1999). But the long wavelength emission can efficiently be boosted if the disc gets into a warped configuration (Terquem & Bertout, 1993; Miyoshi et al., 1995; Bachev, 1999).

Beyond a certain radius, self-gravity becomes important and reduces the disc thickness such that $\frac{d \ln h}{d \ln R} < 0$

¹ The author plans to make the executable available to the community. In the meanwhile, vertical structure computations may be performed on special request.

(Sakimoto & Coroniti, 1981; Shore & White, 1982; Cannizzo & Reiff, 1992; Liu, Xie & Ji, 1994; Huré et al., 1994a; Huré, 1998). As we shall see below, the same effect is observed from vertical structure computations. It means that outer parts should not receive directly light emitted at the center, contrary to the inner parts. Note that a disc is generally not isolated but embedded into a "warm" environment which may in turn heat it up. Discs in YSO are surrounded by an envelope of gas and dust resulting from the cloud core collapse (Mundy, Looney & Welch, 2000; Chick & Cassen, 1997; D'Alessio, Calvet & Hartmann, 1997). In the case of AGN, clouds moving above the disc (BLR clouds) can scatter light back onto it (Shields 1977; Collin-Souffrin, 1987; Osterbrock, 1993). It follows that, even outer regions which are not directly exposed to the luminous central source can be substantially irradiated. The disc response to irradiation is a complex problem to solve self-consistently since it depends on many parameters (size and location of the ionizing source(s), shape of the ionizing spectrum, intensity of irradiation, disc flaring angle, surface albedo, disc optical thickness, gas metallicity, etc.) which are neither well known, nor well constrained by current observations. For discs having a large total surface density, mostly the superficial layers are heated up and ionized, and the midplane is essentially not affected (Sincell & Krolik, 1997; Collin & Huré, 1999; Nayakshin, Kazanas & Kallman, 1999; Igea & Glassgold, 1999). Deep structural changes (for instance, a temperature inversion or an iso-thermalization) may however occur in some cases (D'alessio et al. 1998). Although discs should experience some external heating, even in their outermost (self-gravitating) parts, we do not consider irradiation in this paper, for simplicity. So, considering internal viscous heating only, the disc effective temperature, far from the central object, is given by

$$T_{\text{eff}}^4 = \frac{3}{8\pi\sigma} \Omega^2 \dot{M} \quad (24)$$

where \dot{M} is the mass accretion rate.

In the following, we apply the code to the computation of the vertical structure of two different systems subject to vertical self-gravity: circumstellar discs and AGN discs. We restrict to central masses of $1 M_\odot$ and $10^8 M_\odot$ respectively, and we show on a few examples how self-gravity and turbulent pressure which are the main specificities of this model affect the disc structure. Computations are performed discarding any kind of instabilities the disc could undergo. These are stopped when the temperature at the top atmosphere (i.e. $T(H) = (\frac{1}{2})^{1/4} T_{\text{eff}}$) attains 10 K, for both physical and practical reasons.

4.2. Effect of turbulent pressure on the vertical temperature and density stratification: an example

To see clearly the influence of turbulent pressure (see Eq.(10)), we have chosen a simulation with $\alpha = 1$ which

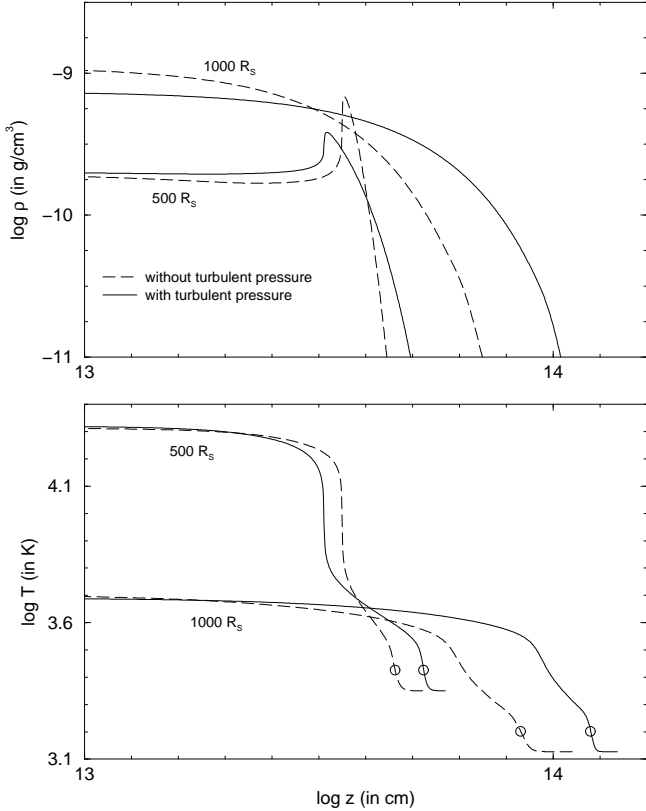


Fig. 2. Effect of turbulent pressure on the distribution of the density (*top*) and temperature (*bottom*) with the altitude z in an AGN disc with $M = 10^8 M_\odot$, $\dot{M} = 10^{-1} M_\odot/\text{yr}$ and $\alpha = 1$ at 500 and 1000 R_S from the center (R_S is the Schwarzschild radius of the black hole). The position of the bottom atmosphere is marked by a circle.

corresponds to the very upper limit regarding supersonic turbulence. In addition, convection and self-gravitation are turned off. Under these circumstances, we have computed the vertical structure with viscosity law ν_1 for an disc around a massive black hole with $M = 10^8 M_\odot$, at two different radii: $R = 500 R_S$ ($R_S = 2GM/c^2$ is the Schwarzschild radius of the black hole) and $R = 1000 R_S$. The accretion rate is $\dot{M} = 10^{-1} M_\odot/\text{yr}$. The temperature and density profiles so obtained are plotted in Fig.(2). We see that turbulent pressure makes the disc thicker, as expected intuitively. Actually, according to Eq.(11), the density gradient is lowered with turbulent pressure and the transition from the ambient medium to the disc interior is softer. The flux gradient depending on the density to a positive power—in the absence of convection at least—, a larger integration range is needed to obtain a zero net flux at the midplane, hence a thicker disc. The effect is specially visible at $R = 1000 R_S$, with a 41% disc thickening (measured on h ; we have 33% on H). The disc flaring therefore increases by the same relative quantity. Since we have not explored the whole parameter space, it is probably easy to find cases where the effect is more

important. The total surface density is almost unchanged (a 2% increase only). At 500 R_S , the disc thickening is less important, about 15%. Note in this example the presence of a density inversion which occurs well below the base of the atmosphere. It tends to be washed out by turbulent pressure, as argued in Sect.2.3.

The way turbulent pressure acts on both the temperature and density at the midplane temperature is however less straightforward and depends intimately on the vertical stratification. For a given effective temperature, a disc with a larger surface density would theoretically have a hotter core. But this happens only in the calculation at 500 R_S , and the effect is very minor.

We have checked that the conclusions derived hereabove are qualitatively unchanged using ν_2 (see Sect. 4.5 for another effect of turbulent pressure). We will not discuss the case of circumstellar discs because values of the α -parameter currently adopted for these systems are rather very low (typically $\alpha \sim 10^{-3} - 10^{-2}$; D’Alessio, Calvet & Hartmann, 1997) and so, no effect of turbulent pressure is indeed observable. This has been verified.

4.3. Effect of the viscosity law: ν_1 versus ν_2

In this paragraph, we show a few differences between ν_1 and ν_2 . Convection is taken into account and turbulent pressure is left aside. The midplane temperature, total surface density, disc thickness and disc mass are plotted versus radius in Fig.(3) for $M = 1 M_\odot$, $\dot{M} = 10^{-7} M_\odot/\text{yr}$ and $\alpha = 10^{-3}$. These parameter values are typical of discs around T-Tauri stars (D’Alessio, Calvet & Hartmann, 1997). The disc mass M^{disc} is

$$M^{\text{disc}}(R) = 2\pi \int_{R_{\text{in}}}^R R' \Sigma_t(R') dR' \neq \pi \Sigma_t R^2 \quad (25)$$

where R_{in} is the inner edge of the disc (unimportant as long as $R \gg R_{\text{in}}$). Results computed without self-gravity are also shown in comparison. We see that, in the non self-gravitating region, differences on the geometrical thickness and midplane temperature are small, the disc being slightly thicker and hotter with ν_1 than with ν_2 . The most important effect is on the surface density and consequently on the disc mass: the ν_1 -prescription leads to slightly more massive disc than the ν_2 -prescription (by a factor ~ 2 here).

We see that the disc is definitely affected by self-gravity from approximately 7 AU whatever the viscosity law (in fact, a little bit less with ν_1 which agrees with the fact that that prescription leads to more massive discs, as long as $M^{\text{disc}} \lesssim M$). Let us remind that the importance of self-gravity can be measured by the quantity (see Eq.(5))

$$\zeta(R, z) = \frac{4\pi G \Sigma(R, z)}{\Omega^2 z} \quad (26)$$

which remains finite at $z = 0$ as a Taylor expansion shows. It follows that a "natural" definition for the limit between

the standard disc and the self-gravitating disc can be $\zeta = 1$ at the midplane (if $\zeta > 1$ then the disc contribution to gravity exceeds that due to the central object, vertically).

On the example, the disc thickness goes through a maximum near 10 AU for both viscosity laws. Beyond this radius, the disc becomes thinner and thinner. Regions located farther away can therefore not intercept photons emitted at the center. Interestingly, the temperature and the surface density show very different behaviors. With law ν_1 , the temperature decreases monotonically as R increases, almost as in the absence of self-gravity. So does the total surface density. The midplane density, not shown on graphs, gently increases with the radius. Note that Σ_t (and M^{disc}) are surprisingly not affected by self-gravity. The origin of this insensitivity has not been identified at the time being. Conversely, with law ν_2 , the surface density and the density violently increase with the radius. The disc thickness falls in also very rapidly. The temperature reaches a plateau. In fact, this somewhat "singular" behavior is predicted by the vertically averaged model (Shlosman & Belgelman, 1987; Huré et al. 1994a; Huré, 1998; see also Duschl, Biermann & Strittmatter, 2000). In particular, the temperature T_{sg} at the plateau is mainly fixed by the ratio \dot{M}/α , namely

$$T_{\text{sg}} = \frac{\mu m_{\text{H}}}{k} \left(\frac{4G^2 \dot{M}^2}{9\alpha^2} \right)^{1/3} \\ \simeq 24100 \mu \left(\frac{\dot{M}}{1 \text{ M}_{\odot}/\text{yr}} \right)^{2/3} \alpha^{-2/3} \text{ K} \quad (27)$$

For $\dot{M}/\alpha = 10^{-4} \text{ M}_{\odot}/\text{yr}$ as in Fig.(3), Eq.(27) yields $T_{\text{sg}} \simeq 120 \text{ K}$ (assuming $\mu = 2.33$). Although this value is derived from the one zone model, it is in good agreement with the vertical structure computation which gives a plateau at about 70 K. Note that the drastic increase of the surface density produces an important increase of the disc mass which even exceeds the value obtained with law ν_1 . When $M^{\text{disc}} \gtrsim M$ (this occurs at 23 – 28 AU on the example), the disc becomes very self-gravitating, probably gravitationally unstable (Goldreich & Lynden-Bell, 1965; Shu et al., 1990) and should therefore not be well described with current viscosities (e.g. Lin & Pringle, 1987) nor by steady state solutions (Goldreich & Lynden-Bell, 1965). One reaches here the limit of the model. It is however interesting to note that, asymptotically, there is either a hot very dense solution or a cold more diffuse solution (see Paczyński, 1978).

The same quantities obtained under the same conditions but for an AGN disc with $M = 10^8 \text{ M}_{\odot}$, $\dot{M} = 10^{-2} \text{ M}_{\odot}/\text{yr}$ and $\alpha = 0.1$ are displayed in Fig.(4). Globally, we find similar trends. The singular behavior observed in the previous example with ν_2 inside the self-gravitating regime seems even stronger. Self-gravitation becomes important from about 500 R_{S} . The midplane temperature stabilizes radially at $\simeq 3900 \text{ K}$. This value again compares quite well

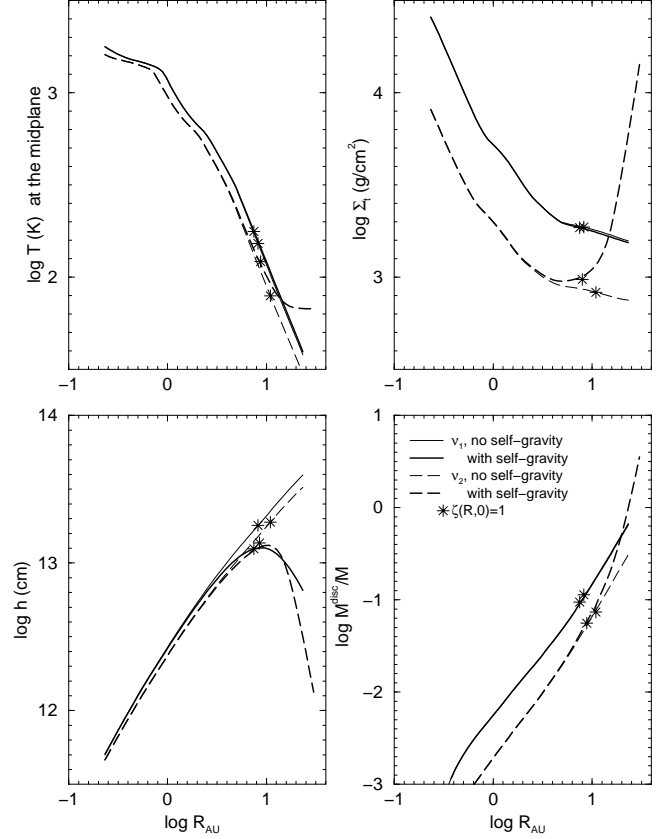


Fig. 3. Midplane temperature, total surface density, geometrical thickness and disc mass versus the radius (in AU) computed with ν_1 (solid lines) and ν_2 (dashed lines) for a disc with $\dot{M} = 10^{-7} \text{ M}_{\odot}/\text{yr}$ and $\alpha = 10^{-3}$ around a one solar mass star.

with Eq.(27) which gives 6600 K (assuming $\mu = 1.27$). The presence of extremely steep surface density and density radial gradients probably means that the assumption made on the disc potential (see Sect. 2.1) is no longer valid. This would be worthwhile to check. The physical picture there is then that of a disc surrounded by a very dense ring (Σ increases by more than one order of magnitude over a relative length $\frac{\Delta R}{R} \sim 15\%$) which contains almost all the disc mass and angular momentum. When $M^{\text{disc}} \gtrsim M$ (beyond a few $10^3 R_{\text{S}}$ for law ν_2), effects of self-gravity are expected to be global, with a change in the rotation law.

All these results require a few comments. First, it is important to note that the effect of self-gravity is slightly underestimated when it is neglected in the computations. This is specially true with law ν_2 . Besides, self-gravity becomes important before ζ reaches unity, like in the one zone model (Huré, 1998). At the inner edge of the self-gravitating disc (that is at $\zeta = 1$ following our definition), the disc mass is much less than the central mass: we find $\frac{M^{\text{disc}}}{M} \sim 10^{-2} - 10^{-1}$ (depending on the viscosity law) in the YSO case, and $\frac{M^{\text{disc}}}{M} \sim 10^{-3}$ in the AGN case. This suggests that low mass discs must not be automatically

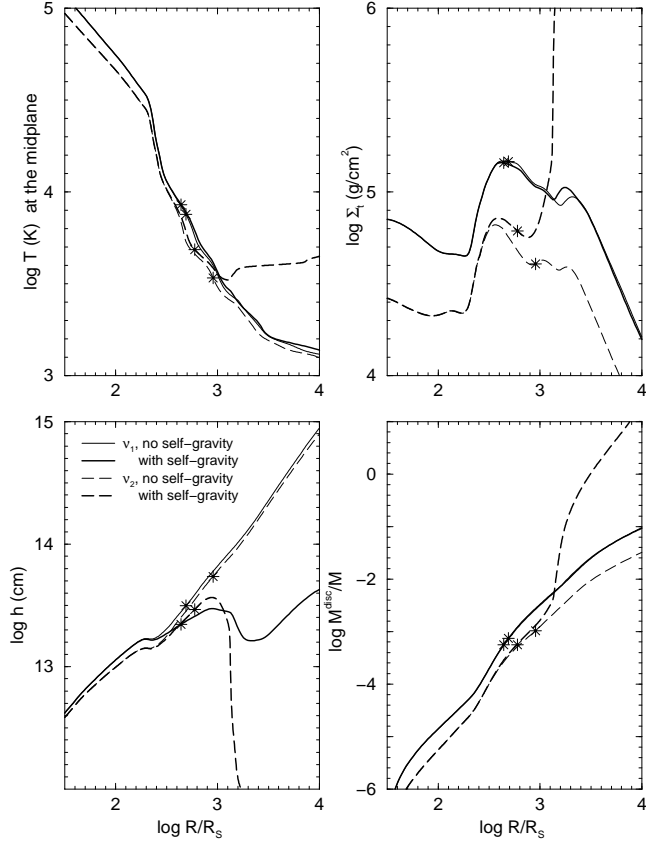


Fig. 4. Same legend as for Fig.(3) but for an AGN disc with $M = 10^8 M_\odot$, $\dot{M} = 10^{-2} M_\odot/\text{yr}$ and $\alpha = 0.1$ (R_S is the Schwarzschild radius of the black hole).

classified as non self-gravitating discs as often asserted. In particular, it is not excluded that T-Tauri discs we observe be subject to vertical self-gravity, despite their relatively low mass (Beckwith et al., 1990).

It has been stated in Sect. 2.4 that the relation between ν_1 and ν_2 is not trivial. In the non self-gravitating parts however, midplane temperatures $T(0)$ show a striking quasi-parallel variation with the radius in logarithmic scales (this is also true for quantities Σ_t and h), which could be attributed to the fact that ν_1 is indeed proportional to ν_2 (or one goes from one solution to the other by a change of α ; see power law solutions for α -discs). To demonstrate that these two viscosity prescriptions are intrinsically different (as suggested by what happens in the self-gravitating regions), we have computed the ratio $\frac{\nu_1}{\nu_2} = \frac{3}{2} \Omega \lambda_p \Gamma_1 / c_s$ with ν_1 , for the examples discussed above. We have chosen two radii, the one lies in the classical disc part, the other is in the self-gravitating part. The results are shown in Fig.(5).

4.4. Example of internal structure: 2D-density maps

We show in Fig.(6) the density field within a circumstellar disc for the same parameter values as in Fig.(3). This

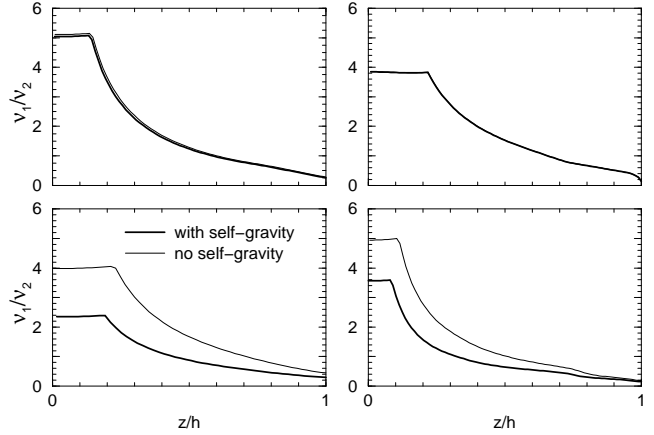


Fig. 5. Ratio ν_1/ν_2 versus z/h using ν_1 for an YSO disc (same parameter values as for Fig.(3)) at 1 AU (*top left*) and 10 AU (*bottom left*), and for an AGN disc (same parameter values as for Fig.(4)) at $100 R_S$ (*top right*) and $500 R_S$ (*bottom right*).

simulation has been carried out using ν_1 and ν_2 as well, including convection, self-gravity and turbulent pressure. We also indicate iso-contours of the temperature, the limit between gas pressure dominated zones and radiative pressure dominated ones, and lines where $\zeta(R, z) = \frac{1}{10}, 1$ and 10 . We notice that the density and the temperature show strong variations in between the midplane to the photosphere's base and we are far from a vertically isothermal, homogenous disc as often considered. Note, specially for viscosity law ν_1 , the re-increase of the midplane density in the radial direction (another density inversion) as self-gravity gains in importance. It is remarkable that self-gravity does not appear suddenly (i.e. on a small radial range) but installs gently and steadily over a very extended domain. For instance, with law ν_2 , it contributes by 10% in the hydrostatic equilibrium near 2 – 4 AU and by 50% at about 7 AU, and all disc quantities are significantly modified over this domain. We see clearly that the disc density is slightly smaller with ν_2 than with ν_1 (same color code for both maps).

We notice that the whole disc is optically very thick, due to its large surface density. It is then likely that a mean external heating should not change noticeably the temperature and density at the midplane. From this point of view, the neglect of irradiation is entirely justified. It is interesting to see that, as long as an α -model can be applied to the Solar Nebula (e.g. Ruden & Pollack, 1991; Pappalouizou & Terquem, 1999; Drouart et al, 1999), our giant planets (displayed on graphs) lie inside the self-gravitating part of the disc (this is true whatever the accretion rate, but depends on the α -parameter; see the next Section). As already noticed (Ruden & Pollack, 1991), this coincidence is somewhat striking and we do not know to what extent self-gravity could have played a role in the process

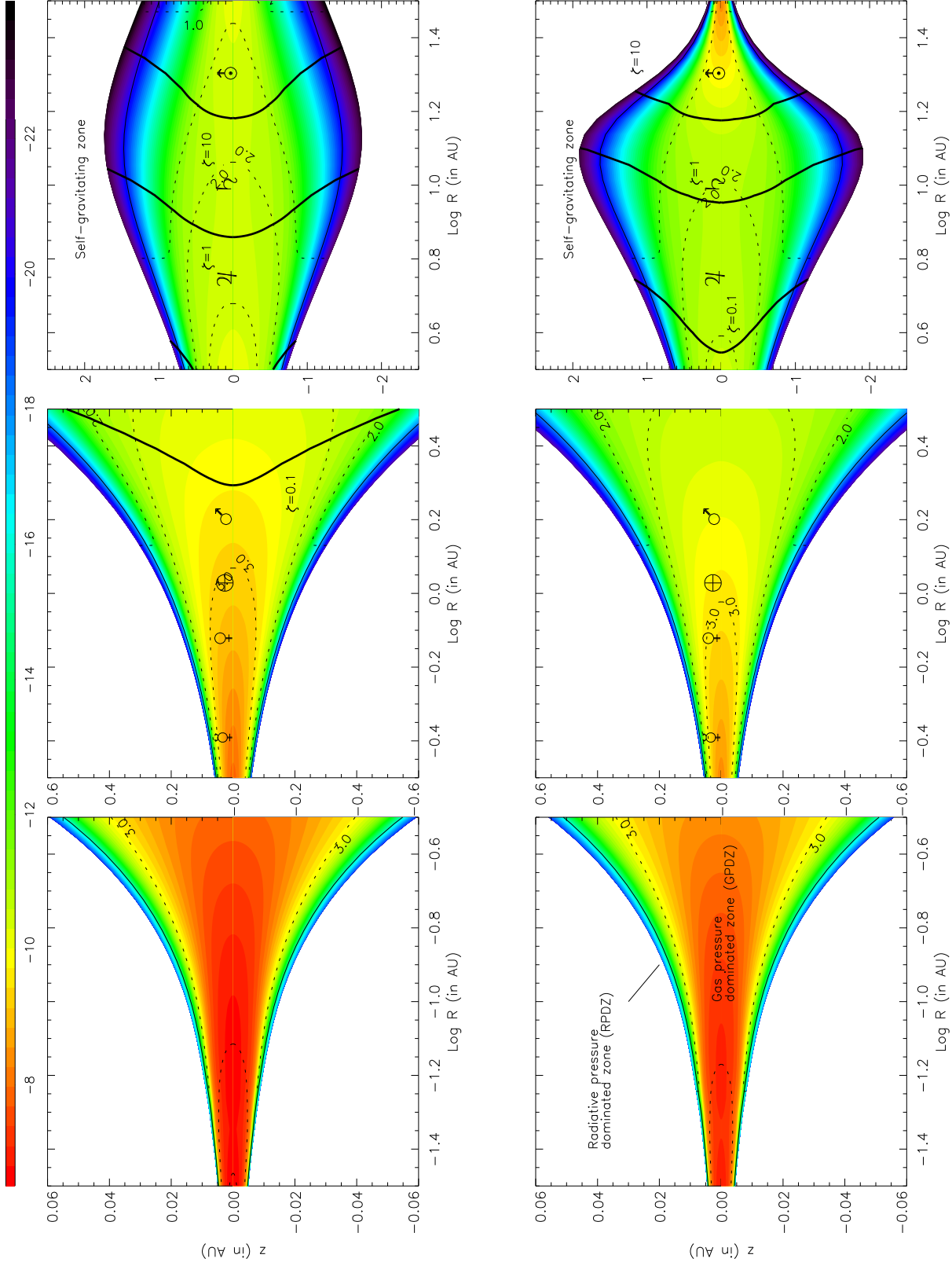


Fig. 6. Density field within a disc surrounding a one solar mass central star, computed with ν_1 (left) and with ν_2 (right). The accretion rate and viscosity parameter are $\dot{M} = 10^{-7} M_{\odot}/\text{yr}$ and $\alpha = 10^{-3}$ respectively. The color code refers to $\log \rho$ (with ρ in g/cm^3) and is the same for both maps. Iso-values of $\log T$ are given in dotted lines. Also indicated in bold lines are contours for $\zeta = 0.1, 1$ and 10 . The limit between the radiative pressure dominated zone (RPDZ) and the gas pressure dominated zone (GPDZ) is marked by a thin plain line.

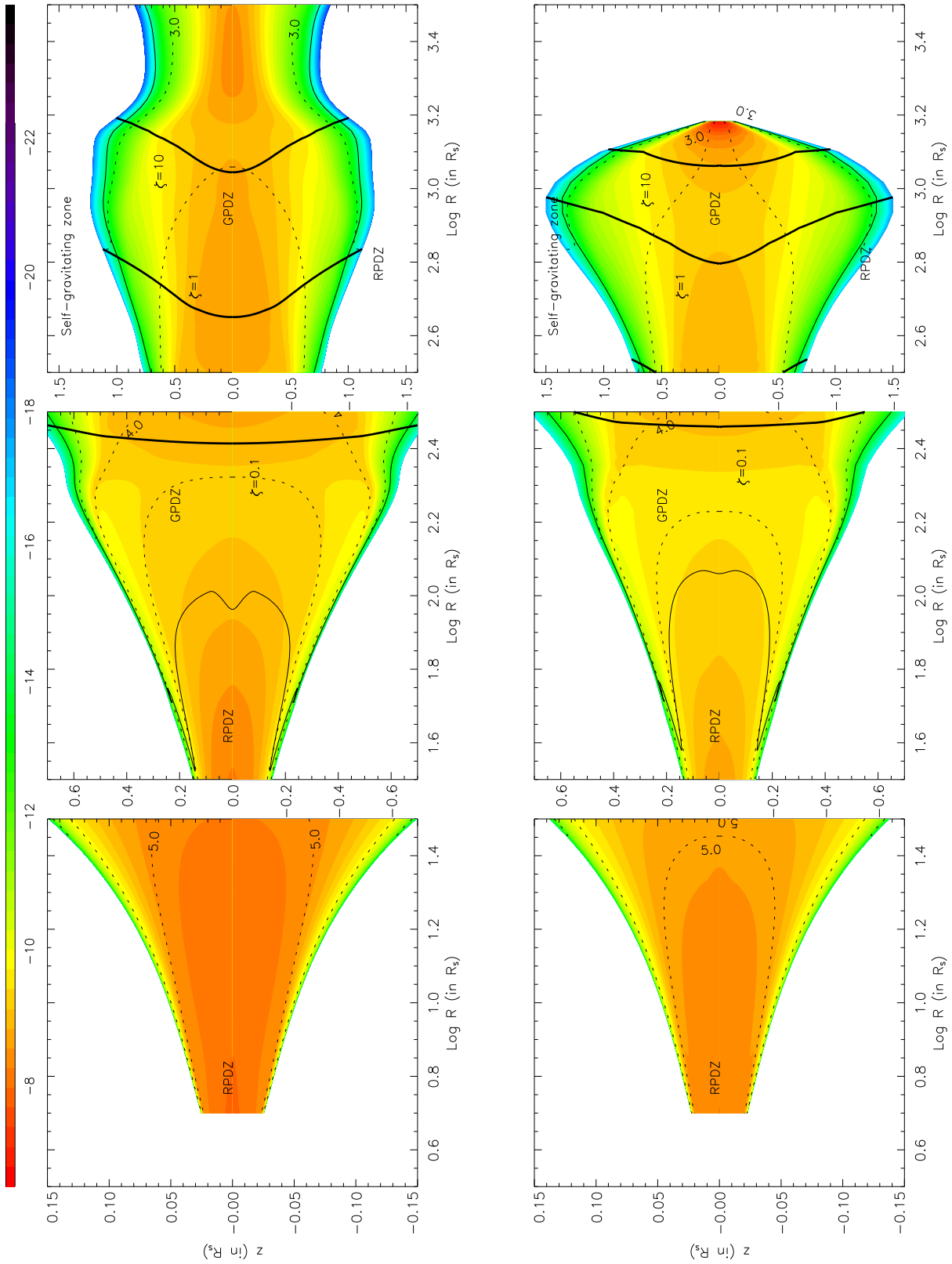


Fig. 7. Same legend (and same color code) as for Fig.(6) but for an AGN disc surrounding a $10^8 M_\odot$ black hole, with $\dot{M} = 10^{-2} M_\odot/\text{yr}$ and $\alpha = 10^{-1}$.

of the formation of outer planet and other objects (Lissauer, 1993).

Similar 2D-maps are displayed in Fig.(7) for an AGN disc with $M = 10^8 M_\odot$, $\dot{M} = 10^{-2} M_\odot/\text{yr}$ and $\alpha = 10^{-1}$, using the same color table. Note the existence of an inner radiative pressure dominated region at $R \lesssim 100 R_S$, common for AGN discs as well as the great steepness of density gradients near the surface which may cause numerical difficulties. Also visible is the density inversion at $R \simeq 160 - 200 R_S$ which has less amplitude and is less extended radially in the presence of convection and turbulent pressure.

4.5. A criterion to check the importance of vertical self-gravity

We see on both Figs.(6) and (7) that $\zeta(R, \infty) < \zeta(R, 0)$ and iso-values of $\zeta(R, z)$ form very curved lines (“diabolo”-shape surfaces in 3D). This is important if one wishes to estimate correctly the position of the self-gravitating regime. For instance, in the case of the law ν_1 discussed in Fig.(6), $\zeta = 1$ in the midplane at 7 AU (we have $450 R_S$ in the AGN case depicted in Fig.(7)) whereas this occurs in the disc atmosphere at about twice the distance.

For many purposes, it is interesting to know the position of the (vertically) self-gravitating disc. That is why we have performed a systematic computation to find the radius R_{sg} satisfying $\zeta(R_{\text{sg}}, 0) = 1$ as a function of the accretion rate, for 4 values of the α -parameter in the range $10^{-3} - 1$, and for $M = 1 M_\odot$ and $M = 10^8 M_\odot$. These parameter values should cover a wide variety of circumstellar discs and AGN discs. The calculations have been performed with ν_2 including convection, self-gravitation, with and without turbulent pressure (the use of ν_1 would systematically give a slightly lower value of R_{sg}). The results are plotted in Fig.(8) for parameter values typical of circumstellar discs. We see that the location of self-gravitating regime is very sensitive to the viscosity parameter. The larger the value of α , the further away the self-gravitating region. Regarding the sensitivity to the accretion rate, there are three different trends. For $\alpha \lesssim 10^{-2}$, the lower \dot{M} , the larger R_{sg} . For $\alpha \sim 0.1$, the dependence is rather weak: $R_{\text{sg}} \approx 27 \pm 3$ AU. For higher values of the viscosity parameter (generally not appropriate to fit properties of observed discs), R_{sg} is an increasing function of \dot{M} . Note also that turbulent pressure, when important, slightly increases R_{sg} ($\sim 12\%$ in the example for $\alpha = 1$ and the highest accretion rate).

Results for AGN discs are shown in Fig.(9). As above, large viscosity parameters imply wider non self-gravitating inner disc (because discs are less dense with large values of the α -parameter), and turbulent pressure pushes further away the self-gravitating regime. For $\alpha \lesssim 10^{-2}$, we have $R_{\text{sg}} \sim 5 - 20 \times 10^{15}$ cm. The sensitivity to the accretion rate remains weak. For higher values of the viscosity parameter and for very low to moderate accretion rates

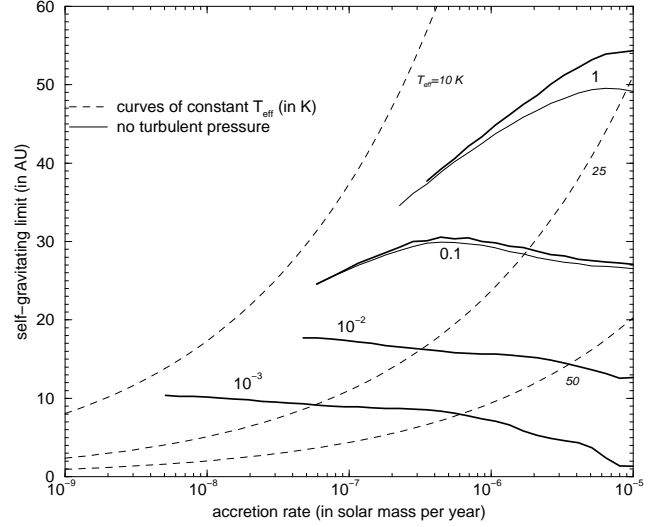


Fig. 8. Inner edge of the self-gravity dominated disc R_{sg} versus the accretion rate for $\alpha = 10^{-3}, 10^{-2}, 0.1$ and 1 with (bold lines) and without turbulent pressure (thin lines). Lines of constant effective temperatures are in dashed lines.

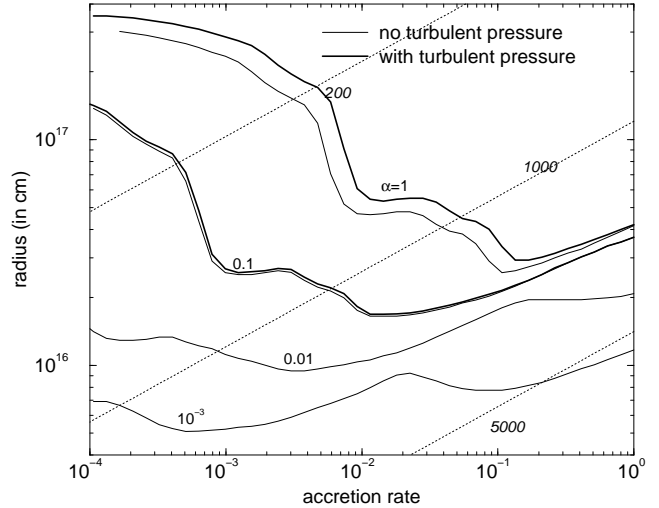


Fig. 9. Same legend as for Fig.(8) but for $M = 10^8 M_\odot$.

($\dot{M} \lesssim 10^{-2} - 10^{-1} M_\odot/\text{yr}$, depending on α), R_{sg} globally decreases as \dot{M} increases. For higher accretion rates, R_{sg} increases as \dot{M} increases and self-gravity is important within the radiative pressure dominated region.

It is important to notify that the “Toomre’s criterion” ($Q_T \equiv \frac{c_s(0)\Omega}{\pi G \Sigma_t} \lesssim 1$) is a helpful tool to trace regions where some gravitational instabilities occur in a stellar disc (Toomre, 1965), but it differs significantly from the criterion derived by Goldreich & Lynden-Bell (1965) for gaseous discs ($Q_{\text{GLB}} \equiv \frac{4Q^2}{\pi G \rho} \lesssim 1$). Besides, Q_T is commonly written in different forms which are not strictly equivalent (e.g., Ruden & Pollack, 1991; Sincell & Krolik, 1997; D’alessio, Calvet & Hartmann, 1997, Papaloizou &

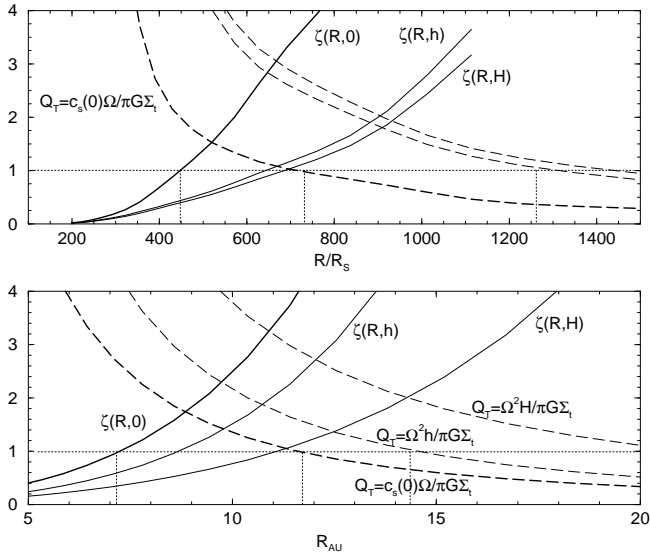


Fig. 10. Comparison between quantity ζ at three different altitudes around the transition $\zeta = 1$ (computed with self-gravity) and the Toomre's parameter Q_T computed (without self-gravity) for three different definitions, for an AGN disc (*top*; same parameter values as in Fig.(7)) and an YSO disc (*bottom*; same parameter values as in Fig.(6)).

Terquem, 1999), specially in a 2D-model. Although these Q -parameters are undisputably related to the ζ -parameter in some ways (for instance, $Q_T \times \zeta(R, \infty) = 2 \frac{c_s(0)}{\Omega H} > 1$ and $Q_{GLB} \times \zeta(R, 0) \simeq 16$), they must be used with care if one wishes to check the importance of self-gravity. They may lead to noticeable over-estimates of R_{sg} , specially if, as it is always the case, the Q_T -parameter is computed from models that discards self-gravity. This is illustrated in Fig.(10) where we have plotted values of ζ at three key altitudes and Q_T versus the radius. It seems therefore preferable to make the check on $\zeta(R, 0)$ rather than on any other quantities, otherwise the importance of self-gravity is under-estimated.

5. Conclusion

In this article, we have presented the equations accounting for the vertical structure of steady state keplerian accretion discs, including simultaneously turbulent pressure, convective transport in the framework of the Mixing Length Theory, and the disc self-gravity within the infinite slab approximation. The emphasis has been placed on outer regions where vertical self-gravity becomes increasingly influential. We have shown that turbulent pressure makes the disc thicker, but it can be neglected if $\alpha \lesssim 0.1$. Also, self-gravity may be important even if the disc mass is very low compared to the central object, contrary to usual assertions. Further, the transition from the classical disc to the self-gravitating disc takes place gradually and so, concerns a large radial domain.

Another important conclusion of this work is that the model of mechanical energy deposition towards the vertical direction is crucial. This is not surprising since viscosity is the source of heating and accretion. Two different behaviors are predicted inside the self-gravitating (and gravitationally unstable) region. On the one hand, the $\alpha\mathcal{P}$ -formalism yields a solution which is asymptotically cold and diffuse, whereas the local version of the standard prescription gives a more "singular" solution, asymptotically hot and dense, which is also predicted by the vertically averaged model. We can imagine that a suitable choice for the function $\nu(z)$ should provide any intermediate solution, meaning that this model for outer regions has almost no predictive power. Although the present stationary keplerian disc model is probably irrelevant to describe the disc structure in its strongly self-gravitating parts, the existence of two asymptotically distinct solutions might indicate that the outer disc can get into, either a flat and cold configuration where fragmentation and formation of individual clouds (Kumar, 1999) and compact objects like planets and stars (Collin & Zahn, 1999) could occur, or into a thick diffuse configuration (a torus) (Paczynski, 1978). Time dependent simulations should shed light on this question.

This study confirms that discs around super-massive black holes are self-gravitating close to the center, beyond a few hundreds Schwarzschild radii, depending on the central mass accretion rate and α -parameter. We have found that the disc surface density remains high when self-gravity dominates and that the disc mass definitely rises outwards. Let us remind that a current problem with the fueling of active nuclei is that the accretion time scale M^{disc}/\dot{M} is usually much too long at large radii, that is why other more efficient mechanisms are invoked (Frank, 1990). However, given the sensitivity of the disc structure to viscosity, it is not excluded that depth dependent viscosity laws other than considered here would lead to smaller surface density distributions, and consequently to shorter accretion time scales. It is therefore important to test other models for the energy deposition along the z -axis as well as other kinds of viscosity prescriptions (Lin & Pringle, 1987; Cannizzo & Cameron, 1988; Richard & Zahn, 1999; see Huré & Richard, 2000).

With accretion rates and values of the viscosity parameter usually considered to model discs in T-Tauri stars, we conclude that our giant planets (if not Jupiter, the other ones) were probably formed within the self-gravitating part of the Solar Nebula (Drouart et al. 1999). This is a fortiori true if these objects experienced any inward migration. More generally, as long as the α -theory may be applied to describe the inner parts of circumstellar discs around forming stars, self-gravity is expected to play a role at about ten AU from the center. This is not incompatible with the discs we observed (Beckwith et al., 1990).

Acknowledgements. I specially thank A. Różańska for many helpful discussions and for providing some reference vertical profiles during the writing and test of the computational code, S. Collin for reading the manuscript. I thank also D. Gautier for highlights on circumstellar discs and the Primitive Solar Nebular, J.-P. Zahn for pointing out the role of turbulent pressure. I am personally grateful to J.M. Hameury for his initiation, some years ago, to the physics of stellar interiors and vertical structure computations. I also thank D. Richard for interesting comments on numerical aspects as well as F. Hersant for widely testing the code. Also, I thank for their hospitality, people at the ITA-Heidelberg where this work was completed, and specially W.J. Duschl.

References

- Abramowicz M.A., Czerny B., Lasota J.P., Szuszkiewicz E., 1988, ApJ, 332, 646
- Abramowicz M.A., Calvani M., Nobili, L., 1980, ApJ, 242, 772
- Adams F.C., Shu F.H., 1986, ApJ, 308, 836
- Aikawa Y., Umabayashi T., Nakano T., Miyam S.M., 1999, ApJ, 519, 705
- Alexander D.R. 1998, private communication
- Alexander D.R., Ferguson J.W., 1994, ApJ, 437, 879
- Artemova I.V., Bisnovaty-Kogan G.S., Björnsson G., Novikov I.D. 1996, ApJ, 456, 119
- Bachev, 1999, A&A, 348, 71
- Beckwith S.V.W., Sargent A.I., Chini R.S., Güsten R., 1990, AJ, 99, 924
- Bell, K.R., Cassen P.M., Klahr H.H., Henning Th., 1997, ApJ, 486, 372
- Bell K.R., Lin D.N.C., 1994, ApJ, 427, 987
- Bertin G., Lodato G., 1999, A&A, 350, 694
- Bertout C., 1989, ARA&A, 27, 351
- Bodo G., Curir A., 1992, A&A, 253, 318
- Boss A., 1996, ApJ, 469, 906
- Brandenburg A., 1998, in *"Theory of black hole accretion discs"*, p61, Eds. Abramowicz, Björnsson & Pringle J.E., Cambridge University Press
- Burgers P., Lamers H.J.G.L.M, 1989, A&A, 218, 161
- Burderi L., King A.R., Szuszkiewicz E., 1998, ApJ, 509, 85
- Camenzind M., Demole F., Straumann N., 1986, A&A, 158, 212
- Cannizzo J.K., 1992, ApJ, 385, 94
- Cannizzo J.K., 1993, in *"Accretion disks ionm compact stellar systems"*, p6, Ed. J.C. Weehler, World Scientific
- Cannizzo J.K., Reiff C.M. 1992, ApJ, 385, 87
- Cannizzo J.K., Cameron A.G.W., 1988, 330, 327
- Cannizzo K.K., Wheeler J.C., 1984, ApJ Sup. Ser., 55, 367
- Collin-Souffrin S., 1987, A&A, 179, 60
- Collin-Souffrin S., Dumont A.-M. 1990, A&A, 229, 292
- Collin S., Zahn J.P., 1999, A&A, 344, 433
- Collin S., Huré J.M., 1999, A&A, 341, 385
- Cox J.P., Giuli R.T., 1968, in *"Principles of stellar structure"*, New York, Gordon and Breach
- Chiang E.I., Goldreich P., 1997, ApJ, 490, 368
- Chick K.M., Cassen P., 1997, ApJ, 477, 398
- Clarke C.J. 1988, MNRAS, 235, 881
- D'Alessio P., Calvet N., Hartmann, 1997, ApJ, 474, 397
- D'Alessio P., Canto G., Calvet N., Lizano S., 1998, ApJ, 500, 411
- D'Alessio P., Cantó J., Hartmann L., Calvet N., Lizano S., 1999, ApJ, 511, 896
- Dörner T., Riffert H., Stauber R, Ruder H., A&A 1996, 311, 69
- De Kool M., Wickramasinghe D., 1999, MNRAS, 307, 449
- Drinkwater M.J., Combes F., Wiklind T., 1996, A&A, 312, 771
- Drouart A., Dubrulle, B., Gautier, D., Robert F., 1999, I, 140, 129
- Dubus G., Lasota J.P., Hameury J.M., Charles P., 1999, MNRAS, 303, 139
- Duley W.W., Williams D.A., in *"Interstellar chemistry"*, London, England and Orlando, FL, Academic Press, 1984
- Duschl W.J, Strittmatter P.A., Biermann P.L., 2000, in press
- Duvert G. et al., 1998, A&A, 332, 867
- El-Khoury Walid, Wickramasinghe D., 1999, MNRAS, 303, 380
- Eriguchi Y., Müller, 1991, 248, 435
- Falcke H., 1998, Rev. Mod. Astr., 11, Schielicke R.E. ed.
- Frank A., 1998, in *"Accretion processes in astrophysical systems: some like it hot"*, Proceedings of the 8th AIP Conference, Ed. S.T. Holt, Kallman T.R., 513
- Frank J., King A., Raine D. 1992, in *"Accretion power in astrophysics"*, 2nd Ed., Cambridge Uni. Press.
- Fukue J., 1992, PASJ, 44, 663
- Goldreich P., Linden-Bell D. 1965, MNRAS, 130, 97
- Guilloteau S., Dutrey A., 1998, A&A, 339, 467
- Güsten R., Chini R., Neckel T., 1984, 138, 205
- Hameury J.M. et al., 1998, MNRAS, 298, 1048
- Hashimoto M., Eriguchi Y., Müller E., 1995, A&A, 297, 135
- Henning & Stognienko R., 1996, A&A 311, 291
- Herrnstein J.R. et al., 1999, Nature, 400, 539
- Hersant F., Gautier D., Huré J.M., 2000, in preparation
- Hubeny I. 1990 ApJ, 351, 632
- Hubeny I., Hubeny V., 1998, ApJ, 505, 558
- Hunter C., 1963, MNRAS, 126, 23
- Huré J.M., Collin-Souffrin S., Le Bourlot J., Pineau des Forêts G. 1994a, A&A, 290, 19
- Huré J.M., Collin-Souffrin S., Le Bourlot J., Pineau des Forêts G. 1994b, A&A, 290, 34
- Huré J.M. 1997, *"Accretion processes in astrophysical systems: some like it hot"*, Proceedings of the 8th AIP Conference, Ed. S.T. Holt, Kallman T.R., 137
- Huré J.M. 1998, A&A, 337, 625
- Huré J.M., Richard D., to appear in *"AGN in their cosmic environment"*, Eds. B. Rocca-Volmerange, Sol H., EDPS Conference Series in Astronomy & Astrophysics
- Huré J.M., Richard, Zahn J.P., 2000, in preparation
- Igea J., Glassgold E, 1999, ApJ, 518, 848
- Kenyon S.J., Hartmann L., 1987, ApJ, 323, 714
- Kenyon S.J., Yi I., Hartmann L., 1996, ApJ, 462, 439
- Kippenhahn R., Weigert A., 1990, in *"Stellar structure and evolution"*, Springer Berlin
- Kumar P., 1999, ApJ, 519, 599
- Lasota J.-P., Hameury J.-P. 1998, in *"Accretion processes in astrophysical systems: some like it hot"*, Proceedings of the 8th AIP Conference, Ed. S.T. Holt, Kallman T.R., 351
- Laughlin G., Różyczka M., 1996, ApJ, 456, 279
- Lin D.N.C., Papaloizou J.C.B., 1980, MNRAS, 191, 37
- Lin D.N.C., Pringle J.E., 1987, MNRAS, 225, 607
- Liu B.F., Xie G.Z., Ji K.F., 1994, A&SS, 220, 75
- Lynden-Bell D., Pringle J. 1974 MNRAS, 168, 603
- Lissauer J.J., 1993, ARAA, 31, 129

- Malbet F., Bertout C., 1991, 383, 814
- Maraschi L., Reina C., Treves A., 1976, ApJ, 206, 295
- Masuda N., Nishida S., Eriguchi Y., 1998, MNRAS, 297, 1139
- Meyer F., Meyer-Hodmeister E., 1982, A&A, 106, 34
- Miyoshi M. et al. 1995, Nature, 373, 127
- Mihalas D., 1978, in “*Stellar Atmospheres*” (San Fransisco: Freeman)
- Milsom J. A., Chen X., Taam R. E., 1994, ApJ, 421, 668
- Mineshige S., Osaki Y., 1983, PASJ, 35, 377
- Mineshige S., Tuchman Y., Wheeler J.C., 1990, ApJ, 359, 176
- Mineshige S., Umemura. M, 1997, ApJ, 480, 167
- Mundy L.G., Looney L.W. and Welch, W.J., 2000, in “*Protostars and Planets IV*”, Ed. Mannings V., Boss A.P., Russell S.S. (Tucson: University of Arizona Press), in press
- Narayan R., Madevan R., Quataert E., 1998, in “*The Theory of Black Hole Accretion Disks*”, Eds. Abramowicz M.A., Bjornsson G. & pringle J.E., Cambridge Uni. Press
- Nayakshin S., Kazanas D., Kallman, T., 1999, AAS, 195, 3903
- Osterbrock D.E., 1993, Ap.J., 404, 551
- Paczynski B. 1978, AcA, 28, 91
- Papaloizou J.C.B., Terquem C., 1999, ApJ, 521, 823
- Pojmański G., 1986, Acta A, 36, 69
- Pollack J.B. et al. 1994, Ap. J., 421, 615
- Press W.H., Teukolsky S.A., Vetterling W.T., Flannery B.P., 1992, in “*Numerical recipes in FORTRAN. The art of scientific computing*”, Cambridge: University Press, p727
- Pringle J. 1981 ARA&A, 19, 137
- Pringle J.E., Rees M.J. 1972, Astr. Ap., 21, 1
- Pudritz R.E. et al., 1996, ApJ, 470, L123
- Richard D., Zahn J.-P. 1999, A&A, 347, 734
- Ross R.R., Fabian A.C., Mineshige S., 1992, MNRAS, 258, 189
- Robinson E.L., Marsh T.R., Smak J.I., 1993, in “*Accretion disks ionm compact stellar systems*”, p75, Ed. J.C. Weehler, World Scientific
- Rózańska A., Czerny B., Zycki P.T., Pojmański G., 1999, MNRAS, 305, 481
- Rózańska A. 1998, private communication
- Ruden S.P., Pollack J.B., 1991, ApJ, 375, 740
- Sakimoto P.J., Coroniti F.V. 1981, ApJ, 247, 19
- Sanders D.B. et al. 1989, ApJ, 347, 29
- Sandqvist Aa., 1999, A&A, 343, 367
- Seaton M.J., Yan Y., Mihalas D., Pradhan A.K., 1994, MNRAS, 266, 805
- Shakura N.I., Sunyaev R.A. 1973, A&A, 24, 337
- Shaviv G., Wehrse R., 1991, A&A, 251, 117
- Shepherd D.S., Kurtz S.E., 1999, ApJ, 523, 690
- Shields G.A., 1977, Ap.J. Let., 18, 119
- Shlosman I., Begelman M.C. 1987, Nature, 329, 810
- Shore S.N., White R.L. 1982 ApJ. 256, 390
- Shu F. H., Tremaine S., Adams F. C., Ruden S. P., 1990, ApJ, 358, 495
- Siemiginowska A., Czerny B., Kostyunin V. 1996, ApJ, 458, 491
- Sincell M., Krolik J., 1997, ApJ, 476, 605
- Smak J., 1984, Acta Astron., 34, 161
- Stahler S.W., 1983, ApJ, 268, 155
- Störzer H., 1993, ApJ, 271, 25
- Terquem C., Bertout C., 1993, A&A, 274, 291
- Toomre A. 1964, ApJ, 139, 1217
- Thé P.S., Molster F.J., 1994, A&SS, 212, 125
- Tuchman Y., Mineshige S., Wheeler J.C., 1990, ApJ, 359, 164
- Voit G.M., 1991, ApJ, 379, 122
- Wehrse R., Störzer H., Shaviv G., 1993, A&SS, 205, 163
- Zeppen C.J., 1998, private communication
- Zdziarski A.A. 1986, ApJ, 305, 45

Appendix A: Treatment for convection in the presence of self-gravitation

Convection is treated with in the framework of the Mixing Length Theory (MLT) (Cox & Giuli, 1968). It is modified in order to include turbulent pressure in the determination of the pressure scale height, and self-gravitation. Following the original version of the MLT, we neglect the variation of gravity with the altitude z . It is likely that turbulent pressure modify significantly the velocity of rising elements within convectively unstable zones, specially if the α -parameter is close to unity, but this effect is not considered here. The total pressure height scale writes

$$\lambda_p \equiv -\frac{dz}{d \ln (P + p_t)} > 0 \quad (\text{A.1})$$

where P is the total (gas plus radiation) pressure and p_t is the turbulent pressure. This expression being singular at the midplane ($\lambda_p \rightarrow \infty$) (see Eq.(5)), the pressure scale height is usually limited to the disc thickness

$$\bar{\lambda}_p = \text{Inf} \left[h, \frac{P + p_t}{\rho (\Omega^2 z + 4 \pi G \Sigma)} \right] \quad (\text{A.2})$$

where ρ is the gas density, Ω is the rotation frequency, Σ is the surface density and h is the altitude of the bottom atmosphere.

According to Eq.(7), the temperature gradient is

$$\frac{d \ln T}{dz} = -\frac{\nabla}{\lambda_p} \quad (\text{A.3})$$

where the actual gradient $\nabla \equiv \frac{d \ln T}{d \ln P}$ depends on the adiabatic gradient $\nabla_{\text{ad}} = \left(\frac{d \ln T}{d \ln P} \right)_{\text{ad}}$ (computed from the EOS; see the next Section) with respect to the fictitious radiative gradient ∇_r defined as

$$\nabla_r = \frac{3 \rho \kappa F \bar{\lambda}_p}{16 \sigma T^4} \quad (\text{A.4})$$

where F is the flux to be transported upwards and κ is a grey absorption coefficient which must approach the Rosseland mean κ_R at great optical depth (see Sect. 3.1).

When $\nabla_r \leq \nabla_{\text{ad}}$ (i.e. in convectively stable zones), heat is transported through radiation only and we have $\nabla = \nabla_r$. Conversely, when $\nabla_r > \nabla_{\text{ad}}$, ∇ is computed from

$$\nabla = (1 - x^3) \nabla_r + x^3 \nabla_{\text{ad}} \quad (\text{A.5})$$

where x is the real root of the third degree equation

$$\frac{9}{4} \mathcal{B}^2 x^3 + \mathcal{B} x^2 + x - \frac{9}{4} \mathcal{B}^2 = 0 \quad (\text{A.6})$$

with

$$\mathcal{B} = \left[\frac{4}{9} \mathcal{A}^2 (\nabla_r - \nabla_{\text{ad}}) \right]^{1/3} \quad (\text{A.7})$$

and

$$\mathcal{A} = \frac{1}{48 \sqrt{2} \sigma} \frac{c_p \kappa_R \alpha_{\text{MLT}}^2 \lambda_p^2}{T^3} \sqrt{\frac{\rho^5}{P}} (\Omega^2 z + 4 \pi G \Sigma) \quad (\text{A.8})$$

where α_{MLT} is the mixing length parameter ($\alpha_{\text{MLT}} = 1.5$ here) and c_p is the constant pressure specific heat capacity.

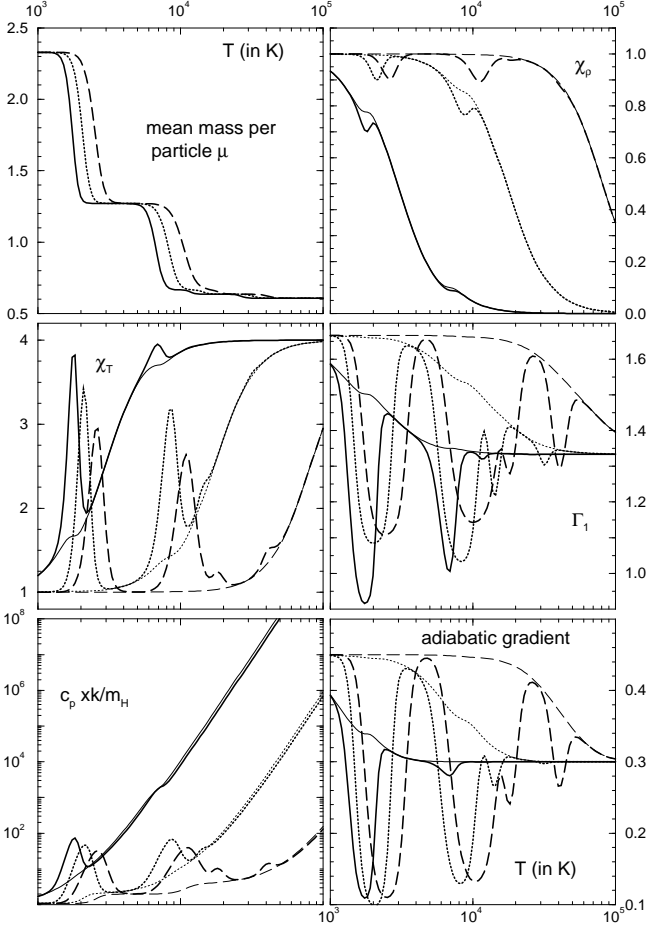


Fig. A.1. Thermodynamic coefficients μ , χ_ρ , χ_T , c_p , Γ_1 and ∇_{ad} computed at thermal equilibrium for a hydrogen-helium mixture with elementary abundances H:He=1: $\frac{1}{10}$ for $\log \rho = -12$ (plain lines), $\log \rho = -10$ (dotted lines) and $\log \rho = -8$ (dashed lines). Raw data are in bold. For μ , χ_ρ and χ_T , the difference between raw data and the high precision fitting formula given in the Appendix (Sect. B1) is not visible. For all coefficients, thin lines are obtained from low precision approximate expressions (see the Appendix, Sect. B2).

Appendix B: Notes on the EOS and related quantities

B.1. High precision fitting formula for μ as functions of the temperature and density — χ -coefficients

Within the assumption of LTE, the pressure of a mixture of radiation and ideal gas undergoing atomic ionization molecular dissociation is given by Eq.(5). In particular, the mean mass per particle μ , in units of the proton mass, is defined as

$$\mu = \frac{\sum_i m_i p_i}{m_H \sum_i p_i} \quad (\text{B.1})$$

where m_i and p_i are respectively individual mass and partial pressure of the chemical compounds, and the sum

Table B.1. Coefficients and functions required to compute $\mu(\rho, T)$ according to Eq.(B.2). Note that $\delta_1 + \dots + \delta_4 = 0.618$ (fully ionized helium), and $\delta_0 - (\delta_1 + \dots + \delta_4) = 2.373$ (fully molecular gas).

| i | δ_i |
|-----|------------|
| 0 | +1.4955 |
| 1 | -0.5400 |
| 2 | -0.3075 |
| 3 | -0.0160 |
| 4 | -0.0140 |

| i | θ_i |
|-----|--|
| 1 | $3.93741 + 0.086042 \log \rho + 0.0023141 \log^2 \rho$ |
| 2 | $4.74029 + 0.116375 \log \rho + 0.0033417 \log^2 \rho$ |
| 3 | $5.07036 + 0.132245 \log \rho + 0.0041041 \log^2 \rho$ |
| 4 | $5.16110 + 0.082767 \log \rho + 0.0017907 \log^2 \rho$ |

| i | Δ_i |
|-----|--|
| 1 | $0.18303 + 0.020252 \log \rho + 0.0007430 \log^2 \rho$ |
| 2 | $0.25730 + 0.030207 \log \rho + 0.0011254 \log^2 \rho$ |
| 3 | $0.09435 + 0.006747 \log \rho + 0.0001561 \log^2 \rho$ |
| 4 | $0.10794 + 0.009201 \log \rho + 0.0002583 \log^2 \rho$ |

extends over the total number of compounds, including electrons. We have computed equilibrium abundances for a mixture of hydrogen and helium (H:He=1: $\frac{1}{10}$) only as function of ρ and T (see Huré, 1998). Data relative to the EOS so obtained are plotted versus the temperature in Fig.(A.1) for three values of the gas density. In particular, the resulting function $\mu(\rho, T)$ has then been fitted with great accuracy by the following expression

$$\mu^{\text{fit}} = \delta_0 + \sum_{i=1,4} \delta_i \tanh \Phi_i, \quad (\text{B.2})$$

with

$$\Phi_i = \frac{\log(T) - \theta_i}{\Delta_i} \quad (\text{B.3})$$

where coefficients δ_i and τ_i and Δ_i are listed in Tab.(B.1). Hyperbolic functions account successively for the transitions H₂/HI, HI/HII, He/HeI and HeI/HeII. Relative errors on raw data $\frac{\Delta\mu}{\mu} = \frac{\mu^{\text{fit}} - \mu}{\mu}$ are displayed in Fig.(B.1) and never exceed 4 % over the whole domain of temperature and density. Besides, the standard deviations with respect to raw data are less than 1.3 %. We have tried to fit the residuals with a few Gaussians, but no major improvement has been obtained. Note that, by construction, the fitting formula shows no singular behavior at high of low densities and temperature. The fit can be used for a cosmic gas without producing large errors (the effect of heavy elements on the EOS is very weak as long as $Z \ll X$).

The temperature and density exponents of the total pressure are respectively given by

$$\chi_T = \left(\frac{\partial \ln P}{\partial \ln T} \right)_\rho = 4(1 - \beta) + \beta \left[1 - \left(\frac{\partial \ln \mu}{\partial \ln T} \right)_\rho \right] \quad (\text{B.4})$$

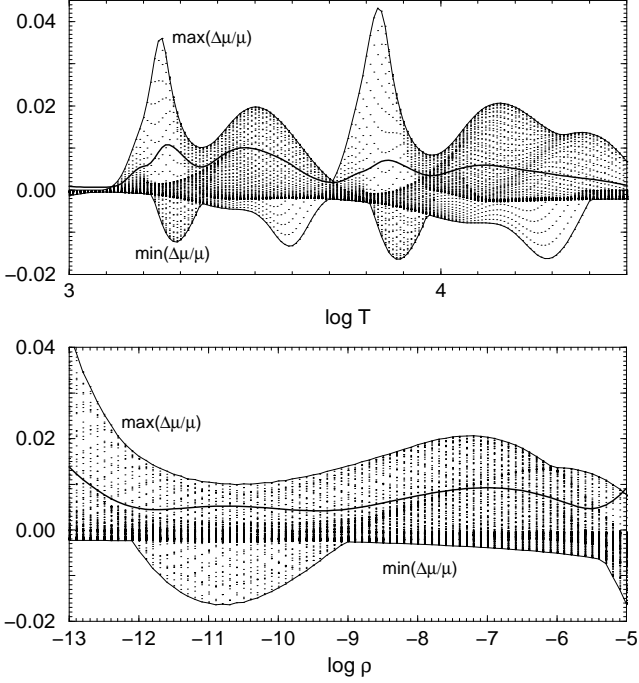


Fig. B.1. Relative error on the mean mass per particle between raw data and fitted values, versus $\log T$ (*upper panel*) and versus $\log \rho$ (*lower panel*). The standard deviation is plotted in bold line.

and

$$\chi_\rho = \left(\frac{\partial \ln P}{\partial \ln \rho} \right)_T = \beta \left[1 - \left(\frac{\partial \ln \mu}{\partial \ln \rho} \right)_T \right] \quad (\text{B.5})$$

where β is the ratio of gas pressure to total (gas plus radiation) pressure. It follows from Eq.(B.2)

$$\begin{aligned} \chi_T &= \frac{\beta}{\mu \log 10} \sum_{i=1,4} \frac{\delta_i}{\Delta_i} (1 - \tanh^2 \Phi_i) \\ &+ \beta(1 - \delta_0) + 4(1 - \beta) \end{aligned} \quad (\text{B.6})$$

and

$$\begin{aligned} \chi_\rho &= \frac{\beta}{\mu \log 10} \sum_{i=1,4} \frac{1 - \tanh^2 \Phi_i}{\delta_i} \left(\frac{d\theta_i}{d \log \rho} \right)_T \\ &+ \beta(1 - \delta_0) \end{aligned} \quad (\text{B.7})$$

and the precision with respect to raw data is also of the order of a few percents.

B.2. Low precision expressions for coefficients χ_T , χ_ρ , ∇_{ad} , Γ_1 and c_p

The adiabatic gradient ∇_{ad} , heat capacity at constant pressure c_p and adiabatic exponent Γ_1 are respectively defined by

$$\nabla_{\text{ad}} = \left[\chi_T + \frac{\chi_\rho}{\chi_T} \left(\frac{\partial U}{\partial \ln \rho} \right)_T \frac{\rho}{P} \right]^{-1} \quad (\text{B.8})$$

where U is the specific internal energy of gas and radiation,

$$c_p = \frac{\chi_T P}{\chi_\rho \rho T \nabla_{\text{ad}}} \quad (\text{B.9})$$

and

$$\Gamma_1 = \frac{\chi_\rho}{1 - \chi_T \nabla_{\text{ad}}} \quad (\text{B.10})$$

Since disc models are still very uncertain, one may use, as a first approximation, low precision expressions for all coefficients related to the EOS discarding changes in the internal energy due to ionizations and dissociations, for instance

$$\chi_\rho \sim \beta \quad (\text{B.11})$$

$$\chi_T \sim 4 - 3\beta \quad (\text{B.12})$$

and then

$$\nabla_{\text{ad}} \sim \frac{1}{4 - 3\beta + \frac{12\beta}{4-3\beta} \left(1 - \frac{21}{24}\beta \right)}, \quad (\text{B.13})$$

$$c_p \sim \left(\frac{4 - 3\beta}{\beta^2} \right) \frac{1}{\mu \nabla_{\text{ad}}} \frac{k}{m_{\text{H}}} \quad (\text{B.14})$$

and

$$\Gamma_1 \sim \frac{\beta}{1 - (4 - 3\beta) \nabla_{\text{ad}}} \quad (\text{B.15})$$